

Structure and dynamics in protic ionic liquids: A combined optical Kerr-effect and dielectric relaxation spectroscopy study

David A. Turton,^{*a} Thomas Sonnleitner,^b Alex Ortner,^c
Markus Walther,^c Glenn Hefter,^d Kenneth R. Seddon,^e Simona Stana,^e
Natalia V. Plechkova,^e Richard Buchner^b and Klaas Wynne^a

Received 1st April 2011, Accepted 1st June 2011

DOI: 10.1039/c1fd00054c

The structure and dynamics of ionic liquids (ILs) are unusual due to the strong interactions between the ions and counter ions. These microscopic properties determine the bulk transport properties critical to applications of ILs such as advanced fuel cells. The terahertz dynamics and slower relaxations of simple alkylammonium nitrate protic ionic liquids (PILs) are here studied using femtosecond optical Kerr-effect spectroscopy, dielectric relaxation spectroscopy, and terahertz time-domain spectroscopy. The observed dynamics give insight into more general liquid behaviour while comparison with glass-forming liquids reveals an underlying power-law decay and relaxation rates suggest supramolecular structure and nanoscale segregation.

1 Introduction

Protic ionic liquids (PILs) have particular importance due to their ongoing development as electrolytes for advanced fuel cells,^{1–5} in addition to a wide range of potential applications including as acidic catalysts. An understanding of structural properties and dynamics are crucial to the full realisation of such applications and there is increasing interest in the presence of nanostructure.^{6,7} Femtosecond optical Kerr-effect (OKE) and dielectric relaxation spectroscopies are both highly sensitive probes of low-frequency diffusional and librational motions.^{8–10} By comparing OKE spectra with dielectric spectra (that cover a range extended to 10 THz, by combining dielectric relaxation spectroscopy (DRS) with time-domain terahertz and FTIR spectroscopies) we recently identified the mesoscopic structure in 1,3-dialkylimidazolium-based room-temperature ionic liquids (RTILs)¹¹ that had been predicted by molecular simulations.^{12,13} This structure appeared even for short-chain RTILs and its presence is critical to understanding their macroscopic properties—viscosity, thermal conductivity, and solute diffusion. Ethylammonium nitrate (EAN) is the most studied, prototypical, PIL.^{14–18}

^aSchool of Chemistry and WestCHEM, University of Glasgow, Glasgow, G12 8QQ, UK. E-mail: david.turton@glasgow.ac.uk; klaas.wynne@glasgow.ac.uk

^bInst. Phys. and Theor. Chemistry, Uni. Regensburg, 93040 Regensburg, Germany. E-mail: Thomas.Sonnleitner@chemie.uni-regensburg.de; Richard.Buchner@chemie.uni-regensburg.de

^cDepartment of Molecular and Optical Physics, Albert-Ludwigs-Universität Freiburg, 79104 Freiburg, Germany. E-mail: alex.ortner@email.de; walther@physik.uni-freiburg.de

^dChemistry Department, Murdoch University, Murdoch, W.A. 6150, Australia. E-mail: g.hefter@murdoch.edu.au

^eQUILL, Queen's University, Belfast, BT9 5AG, UK. E-mail: quill@qub.ac.uk

For EAN and propylammonium nitrate (PAN) the presence of nanoscale segregation is controversial. It has been suggested recently that the ability of each ion to form multiple hydrogen bonds promotes a heterogeneous structure,¹⁶ similar to that of water,¹⁷ and that the hydrogen bond network has on average one H-bond donor and acceptor position free.¹⁹ Small angle neutron scattering (SANS) and large angle X-ray scattering (LAXS) measurements on EAN (and PAN) have been interpreted as evidence of a disordered, locally smectic or sponge-like structure arising partially from electrostatic and hydrogen bonding attractions between the amine nitrogen and the nitrate anion rather than through the ordering of imidazolium ring cations assumed in the imidazolium-based ILs.^{20,21} Further evidence of structure through SANS was shown to be consistent with calculations that imply a nanometre-scale heterogeneity.²² However, computational and X-ray scattering studies have been interpreted to show that low- q scattering peaks do not necessarily imply mesoscale order.²³

The objective of this study is to interpret the transport dynamics of these liquids and identify, if present, structural heterogeneities. Limited measurements of the dielectric spectra have been made previously;^{15,24} this work presents the first continuous spectrum for the entire intermolecular region and is the first OKE study. Wide-band temperature-dependent OKE and dielectric spectra for EAN are presented, with additional OKE measurements for PAN.

OKE spectroscopy measures the derivative over time of the two-point time-correlation function of the anisotropic part of the many-body polarisability tensor Π in the time domain, $S_{\text{OKE}}(t) \propto (d/dt)\langle \Pi_{xy}(t)\Pi_{xy}(0) \rangle$.²⁵ A Fourier-transform deconvolution yields the spectrum and this is equivalent to the Bose–Einstein corrected depolarised Raman spectrum.²⁶ Dielectric spectroscopy similarly measures the derivative over time of the two-point time-correlation function of the dipole moment vector, $S_{\text{DRS}}(t) \propto (d/dt)\langle \mu(t)\mu(0) \rangle$. The two techniques are therefore, to a degree, complementary, but measure the same dynamics resulting in spectra that differ fundamentally only in the amplitudes.²⁷ One exception to this rule is that rotational motions generally appear faster in OKE than in DRS due to the higher symmetry of the polarisability tensor^{28–30} (as discussed below).

2 Experimental

The high viscosities of these strongly interacting liquids result in slow relaxation timescales. Hence, even at room temperature, wide time spans are required to capture the entire intermolecular dynamics. Two OKE set-ups were therefore employed; the faster dynamics were measured using a 7 nJ, 20 fs pulse laser oscillator as described previously,³¹ while—to increase the signal-to-noise of the weaker relaxation measured at longer times—a similar set-up employing a regeneratively-amplified laser (Coherent Legend USX) with a 1 μJ pulse stretched to a duration of *ca.* 1 ps was used. The two measured time-domain signals could be overlapped by greater than an order of magnitude in time allowing accurate concatenation.³² The liquids were contained in a fused-quartz cuvette with a path length of 2 mm. The temperature was controlled by a cryostat (Oxford Instruments, Optistat DN, ± 0.01 K) at sub-ambient temperature or, at higher temperatures, by a lab-built copper cell holder thermostatically controlled to ± 0.1 K.

Broadband dielectric spectra were measured by a frequency-domain reflectometer (Agilent E8364B VNA combined with Agilent 85070E-020 (0.2–20 GHz) and 85070E-050 (0.5–50 GHz) probes)³³ and two waveguide interferometers (IFMs) at 27 to 89 GHz.³⁴ Raw VNA data were corrected for calibration errors with a Padé approximation. For selected samples, two further IFMs at 8.5 to 17.5 GHz³⁴ were used to crosscheck the reliability of the VNA results and showed excellent agreement, within the precision of the instruments. The temperature was controlled to within 0.05 K. A transmission/reflection terahertz time-domain spectrometer (THz-TDS) recorded data from 0.3 to 3 THz,³⁵ with temperature control using

a lab-built cell holder with a precision of ± 0.5 K. The FIR data were recorded from 0.9 to 12 THz on a Bruker Vertex 70 FTIR spectrometer with the liquids held between a pair of polymethylpentene (TPX) windows with a path length of 20 μm in a temperature controlled mount (Harrick TFC-S25 & ATC-024). An average of about 4000 scans was taken for each sample and a background spectrum taken from the windows alone was subtracted. Complex permittivity spectra were then derived by Kramers-Kronig transformation,³⁶ and the data were resampled to a logarithmic frequency scale to match the lower frequency data. These data were then summed to give a nearly continuous spectrum to 10 THz.

Temperature-dependent viscosities were measured for EAN on an Anton-Paar AMVn rolling ball micro-viscometer over the temperature range 5 $^{\circ}\text{C}$ to 100 $^{\circ}\text{C}$ (± 0.05 K).

The EAN sample was prepared in Regensburg by the reaction of equimolar amounts of ethylamine with nitric acid. Water was removed by rotary evaporation followed by lyophilisation. The crude EAN was recrystallized thrice from acetonitrile and the resulting colourless liquid dried at <10 nbar and 50 $^{\circ}\text{C}$ for one week and then stored under nitrogen. The water content determined by coulometric Karl Fischer titration of the final product was 192 ppm. The PAN sample was provided by QUILL at Queen's University Belfast and was prepared by a dropwise addition of concentrated nitric acid to a cold solution of propylamine. The product was dried by lyophilisation for 24 h at 0.38 mbar to give a pale yellow liquid. The water content was <1 wt%. For both samples, purity was confirmed by ^1H NMR spectroscopy.

3 Results and analysis

The OKE and dielectric data for EAN at 25 $^{\circ}\text{C}$ are compared directly in Fig. 1. There are both remarkable differences and similarities in the observed intermolecular dynamics. In both cases, the higher frequencies are dominated by a peak that is familiar from studies of molecular liquids, where it is generally associated with librations (hindered rotational motions). In EAN, surprisingly, the librational band appears to be 2–3 times higher in frequency for the dielectric measurement. At low frequency a strong structural or α -relaxation mode is observed that appears to have a Cole-Davidson (CD) lineshape $S_{\text{CD}}(\omega) = (1 + i\omega\tau)^{-\alpha}$.^{10,24} With respect to

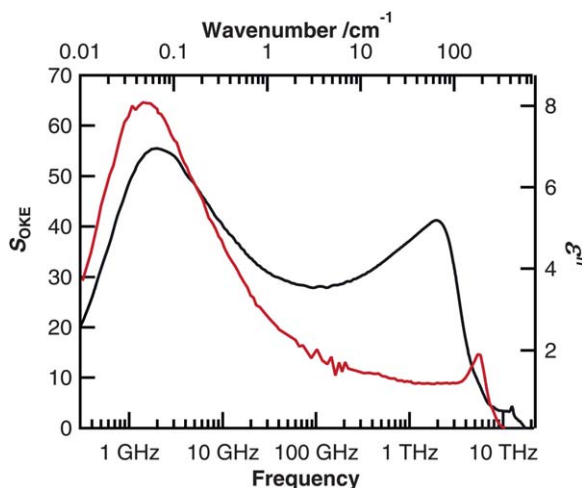


Fig. 1 OKE (black) and dielectric loss, ϵ'' (red) data for EAN at 25 $^{\circ}\text{C}$ (the relative amplitude scaling is arbitrary).

a Debye function, the CD lineshape is asymmetrically broadened by an additional high frequency contribution that, in the time domain, results in an initial power law decay $S \propto t^{1-\alpha}$.³⁷ The CD function is often used as a model of heterogeneous relaxation in deeply supercooled liquids.³⁸ The measured α -relaxation is generally associated with molecular reorientations (*via* the dipole moment or polarisability tensor). Due to the higher symmetry of the polarisability tensor, the (2nd rank) OKE signal relaxes three times faster than the (1st rank) DRS signal in simple cases of diffusional relaxation.^{9,28} However, here the frequencies are quite similar.

For EAN, OKE and DRS data were recorded from 5 °C to 65 °C in steps of 10 °C with the terahertz and FIR data measured at 20 °C steps (Fig. 2).

Arguably, the least well understood region of the spectrum is where the librational modes give way to relaxations. The mode-coupling theory predicts low frequency behaviour above the glass transition T_g but does not yet provide a practical fitting model. In the absence of a more meaningful physical model, such data are typically analysed through phenomenological lineshapes applied in order to parameterise the behaviour allowing comparison to other systems and ideally to give insight into the physical origin of the dynamics. However, the intermolecular dynamics (measured below a few terahertz) often cannot be decomposed into simple functions. Furthermore, data measured in the time domain often are analysed using a different set of models (exponential decay, stretched exponential, power law, *etc.*) to those employed in the frequency domain (Debye, Havriliak-Negami, Gaussian, *etc.*). Several of these functions have no symbolic Fourier transform which leads to confusion as apparently different phenomena are observed. The reconciliation of these two views is overdue.³⁸

As both techniques measure the decay in anisotropy following an impulse, there is an inertial contribution to the signal that occurs through the librational motions. Therefore, the librational process and the relaxation should be somehow combined. This is to some extent achieved when the relaxation is modified by an inertial rise function,^{29,39} in which the inertial frequency is determined by the librational frequencies. However, the spectrum of EAN is typical of viscous liquids in that the librations are well resolved from the α relaxation. The broad region that “connects” the two is poorly understood. In studies of glass-forming liquids, this region has in the time domain been approximated as a series of power laws.⁴⁰ Alternatively, in the frequency domain the sum of a number of Debye, damped harmonic (Brownian), or similar lineshapes are typically employed.^{11,41} Here, there is no actual evidence of individual modes (with the exception of a poorly resolved shoulder in the OKE spectrum close to 1 THz). A solution to this problem appeared with the PAN sample

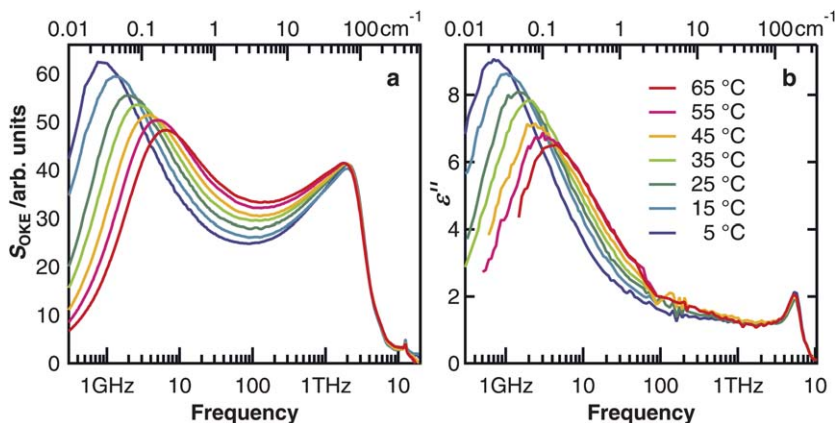


Fig. 2 Spectra for EAN: (a) OKE and (b) dielectric loss measured from 5–65 °C.

that proved to be a relatively good glass former. OKE data were measured down to 140 K allowing the relaxations to be frozen out and the line-shape of the non-diffusional response to be revealed (Fig. 3(a)).

In the time domain, it can be seen that as the temperature falls, the response approaches a line (on logarithmic scales). This is characteristic of a power-law decay, $S \propto t^{-p}$. At 200 K, p is measured at 0.82. At lower temperatures, but above the glass transition, the sample typically crystallised after several minutes preventing reliable measurements of the relaxation, but it appears that p tends to unity, *i.e.* to a logarithmic decay.⁴⁰ In the frequency domain, this appears as a constant loss or white noise response.⁴² A convenient method of generating such a response is given by the Cole-Cole function $S_{CC}(\omega) = 1/(1 + (i\omega\tau)^\beta)$. The Cole-Cole function is a Debye function broadened symmetrically by the exponent β for $0 < \beta < 1$. We have shown previously how this function can be made consistent with spectroscopic dynamics by terminating it in the α relaxation at low frequency, and by applying an inertial rise modification at high frequency.²⁹ In the limit of $\beta \rightarrow 0$, a logarithmic decay results that for the modified function extends appropriately from the librations to the α relaxation (Fig. 4 and 5). This fit was then used as the basis for fitting the temperature dependent data for both the OKE and dielectric measurements.

The fit for the two data sets at 25 °C is shown in Fig. 5. A concise fit was given by a Cole-Davidson function for the α relaxation with the librational modes described by a Gaussian function, the width of which might imply the heterogeneity of the cage structures. The weak mode at ~ 1 THz is fitted by a damped-harmonic oscillator. The logarithmic decay (Cole-Cole function) links the librations to the α relaxation, and is defined by a single amplitude parameter combined with the inertial rise rate and α relaxation time.

The α -relaxation time constants are also shown on an Arrhenius plot in Fig. 6. The viscosity, which extends to 100 °C, is non-Arrhenius and is fitted by the Vogel-Fulcher-Tammann function.^{43,44} The two measures of the α relaxation do appear to be Arrhenius over the measured temperature range, but have activation energies that differ by $\sim 10\%$ (21.7 kJ mol⁻¹ for DRS and 23.9 kJ mol⁻¹ for OKE).

4 Discussion

Both the difference of librational frequencies and, to some extent, the anomalous relaxation rates can be explained simply. The nitrate ion is planar with delocalised

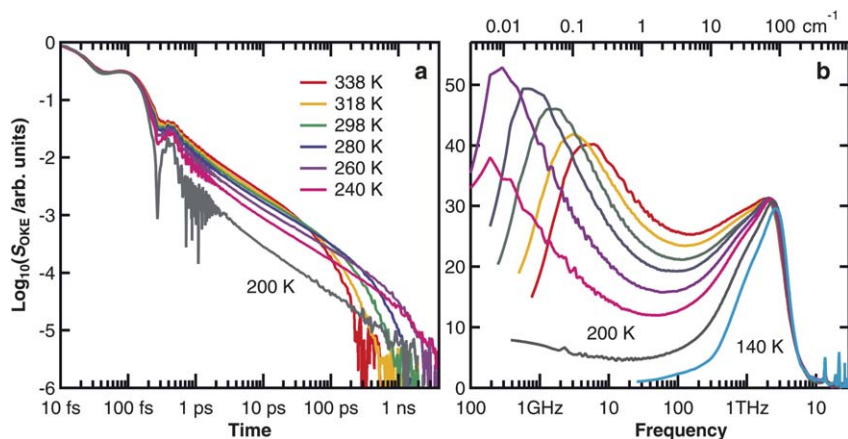


Fig. 3 (a) Time-domain OKE signal for PAN for seven temperatures between 200 K and 338 K. The fast and slow dynamics signals are concatenated at *ca.* 5 ps. (b) The imaginary part of the spectrum is yielded by a Fourier transform deconvolution of (a).

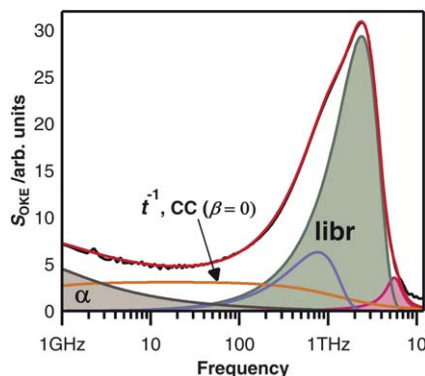


Fig. 4 Fit (red) of the OKE spectrum (black) for PAN at 200 K. CC is the Cole-Cole function with $\beta = 0$ as described in the text.

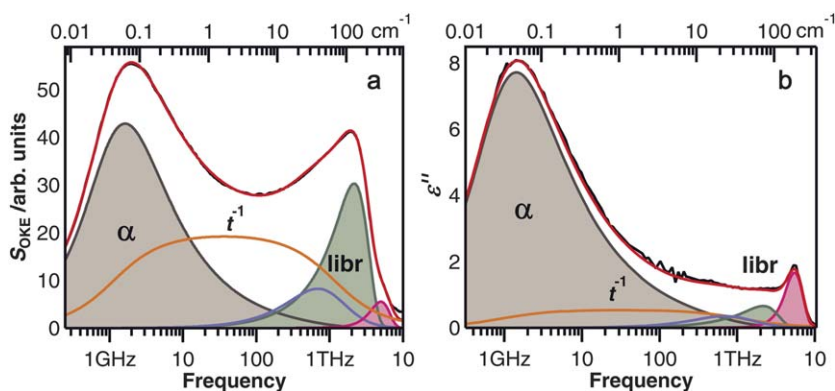


Fig. 5 Fit to (a) the OKE data and (b) the dielectric loss for EAN at 25 °C.

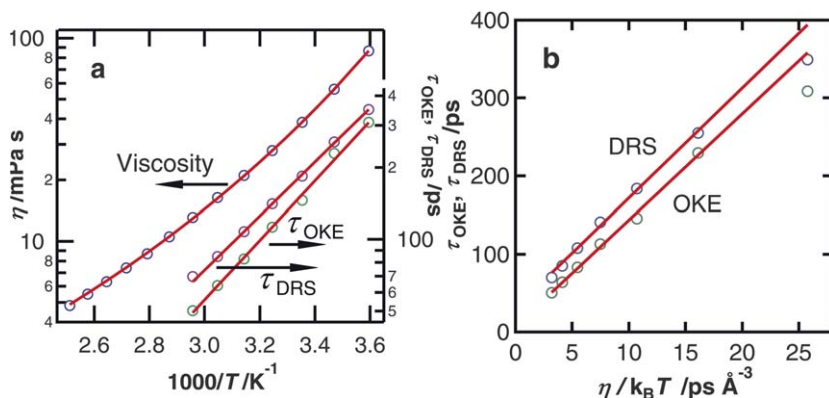


Fig. 6 (a) Arrhenius plot of the alpha relaxation time constant for the fits to both OKE and DRS data for EAN compared to viscosity. (b) Stokes–Einstein–Debye relationship.

π -bonding and an overall negative charge. This results in a highly polarisable ion that has a high degree of anisotropy ($\alpha_{\parallel} \approx 5.6 \text{ \AA}^3$, $\alpha_{\perp} \approx 3.1 \text{ \AA}^3$ ⁴⁵), but no intrinsic dipole moment. Conversely, the alkylammonium ion does have a permanent dipole

moment, and also has a tightly-bound depleted charge system with no aromatic character and is therefore only weakly polarisable. This system therefore has almost perfect complementarity: the dielectric spectrum is sensitive to motions of the cation while OKE is sensitive to the anion. It has been suggested, with reference to DFT calculations,¹⁹ that the two strong bands, at ~ 2 and ~ 6 THz, are directly equivalent to the hydrogen bond bend and stretch of water.²⁸ However, since the dielectric and OKE signals are both primarily sensitive to rotations, the dominant contribution in this region is likely to be librational, in which case the shoulder observed just below 1 THz would be a likely candidate for the hydrogen bond stretch.

Both OKE and dielectric measurements for EAN reveal a well defined α -relaxation mode but there is no evidence of the sub- α mode indicative of mesoscopic structure that is present in the more complex planar imidazolium-based ILs.¹¹ Furthermore, the temperature-dependent data do not reveal a clear change from structured to unstructured as might be expected to appear as a break in the Arrhenius dependence or an anomalous change in the terahertz dynamics.

However, in contrast to single-molecule relaxation, which follows Arrhenius behaviour, the viscosity becomes “super-Arrhenius” at low temperature, even over the limited range of 5–65 °C. This behavior is referred to as “fragile”. Fragility is not unusual in ILs⁴⁴ but this decoupling of viscosity and diffusivity implies a Stokes–Einstein–Debye violation. The super-Arrhenius behaviour is often interpreted as due to the presence of clusters that result in increasing length scales as a liquid is supercooled. However, then it would be usual for the single-molecule dynamics to be similarly affected. The Stokes–Einstein–Debye (SED) expression $\tau_{\text{rot}} = V_{\text{eff}}\eta/k_{\text{B}}T$, relates the rotational relaxation time constant τ_{rot} to viscosity η through the effective molecular volume V_{eff} . Although derived for spherical particles diffusing in a homogeneous fluid, the expression has proven applicable to a much wider range of systems. In Fig. 6(b), τ_{rot} is plotted against $\eta/k_{\text{B}}T$, to yield V_{eff} . Values of *ca.* 15 Å³ are found for both OKE and DRS, but for the latter the additional factor of 3 gives 5 Å³. Corrections can be applied for the molecular aspect ratio and slip or stick conditions³⁶ but this simple estimate suggests that V_{eff} for the ethylammonium ion is underestimated. The active motion for the nitrate ion (in OKE) is out-of-plane rotation and for the alkylammonium ion (in DRS) end-over-end rotation which does not suggest that V_{eff} for the ammonium ion should be particularly small.

The most obvious explanation for these disparities is that the liquid is not a simple one. Rather it is a strongly-interacting cooperatively-relaxing mixture. In particular, it is reasonable to expect that the multiple hydrogen bonds result in relaxation through a molecular jump mechanism as described for water.⁴⁶ The relaxation time is therefore determined, in each case, by the rate of hydrogen bond breaking rather than the diffusional process intrinsic to the SED relation.

The divergence of viscosity from single-molecule diffusivity at low temperatures, visible in Fig. 6(a) and 6(b), is consistent with increasing inhomogeneity due to cluster formation. If so, these clusters do not introduce additional low-frequency modes in either spectrum, which suggests aggregation of the alkyl groups on the cation consistent with the previous experimental observations and simulations of weakly-defined structure. Such aggregates would have zero net dipole moment (if approximately symmetrical), would not result in an appreciable OKE signal due to the very weak polarisability of the cation, and would not significantly influence the relaxation of the nitrate ion, which hydrogen bonds to the $-\text{NH}_3$ site. The degree of aggregation must be low according to the small deviation from Arrhenius behaviour and since the DRS signal is not severely attenuated at low temperature.

Acknowledgements

We are grateful to the EPSRC and DFG for funding.

References

- 1 W. Xu and C. A. Angell, *Science*, 2003, **302**, 422–425.
- 2 M. Yoshizawa, W. Xu and C. A. Angell, *J. Am. Chem. Soc.*, 2003, **125**, 15411–15419.
- 3 J. Le Bideau, L. Viau and A. Vioux, *Chem. Soc. Rev.*, 2011, **40**, 907–925.
- 4 H. Nakamoto and M. Watanabe, *Chem. Commun.*, 2007, 2539–2541.
- 5 S. Y. Lee, A. Ogawa, M. Kanno, H. Nakamoto, T. Yasuda and M. Watanabe, *J. Am. Chem. Soc.*, 2010, **132**, 9764–9773.
- 6 T. L. Greaves, D. F. Kennedy, S. T. Mudie and C. J. Drummond, *J. Phys. Chem. B*, 2010, **114**, 10022–10031.
- 7 T. L. Greaves, D. F. Kennedy, A. Weerawardena, N. M. K. Tse, N. Kirby and C. J. Drummond, *J. Phys. Chem. B*, 2011, **115**, 2055–2066.
- 8 G. Giraud, C. M. Gordon, I. R. Dunkin and K. Wynne, *J. Chem. Phys.*, 2003, **119**, 464–477.
- 9 D. A. Turton, J. Hunger, G. Hefter, R. Buchner and K. Wynne, *J. Chem. Phys.*, 2008, **128**, 161102.
- 10 J. Hunger, A. Stoppa, S. Schrödle, G. Hefter and R. Buchner, *ChemPhysChem*, 2009, **10**, 723–733.
- 11 D. A. Turton, J. Hunger, A. Stoppa, G. Hefter, A. Thoman, M. Walther, R. Buchner and K. Wynne, *J. Am. Chem. Soc.*, 2009, **131**, 11140–11146.
- 12 Y. T. Wang and G. A. Voth, *J. Am. Chem. Soc.*, 2005, **127**, 12192–12193.
- 13 J. Lopes and A. A. H. Padua, *J. Phys. Chem. B*, 2006, **110**, 3330–3335.
- 14 J. N. C. Lopes and L. P. N. Rebelo, *Phys. Chem. Chem. Phys.*, 2010, **12**, 1948–1952.
- 15 M. Kruger, E. Brundermann, S. Funkner, H. Weingartner and M. Havenith, *J. Chem. Phys.*, 2010, **132**, 101101.
- 16 S. Ishiguro, Y. Umebayashi, R. Kanzaki and K. Fujii, *Pure Appl. Chem.*, 2010, **82**, 1927–1941.
- 17 K. Fumino, A. Wulf and R. Ludwig, *Angew. Chem., Int. Ed.*, 2009, **48**, 3184–3186.
- 18 T. L. Greaves and C. J. Drummond, *Chem. Soc. Rev.*, 2008, **37**, 1709–1726.
- 19 S. Zahn, J. Thar and B. Kirchner, *J. Chem. Phys.*, 2010, **132**, 124506.
- 20 R. Atkin and G. G. Warr, *J. Phys. Chem. B*, 2008, **112**, 4164–4166.
- 21 Y. Umebayashi, W.-L. Chung, T. Mitsugi, S. Fukuda, M. Takeuchi, K. Fujii, T. Takamuku, R. Kanzaki and S.-i. Ishiguro, *J. Comput. Chem., Jpn.*, 2008, **7**, 125–134.
- 22 R. Hayes, S. Imberti, G. G. Warr and R. Atkin, *Phys. Chem. Chem. Phys.*, 2011, **13**, 3237–3247.
- 23 C. S. Santos, H. V. R. Annappureddy, N. S. Murthy, H. K. Kashyap, E. W. Castner and C. J. Margulis, *J. Chem. Phys.*, 2011, **134**, 064501.
- 24 H. Weingartner, A. Knocks, W. Schrader and U. Kaatz, *J. Phys. Chem. A*, 2001, **105**, 8646–8650.
- 25 C. J. Fecko, J. D. Eaves and A. Tokmakoff, *J. Chem. Phys.*, 2002, **117**, 1139–1154.
- 26 N. A. Smith and S. R. Meech, *Int. Rev. Phys. Chem.*, 2002, **21**, 75–100.
- 27 G. Giraud and K. Wynne, *J. Chem. Phys.*, 2003, **119**, 11753–11764.
- 28 T. Fukasawa, T. Sato, J. Watanabe, Y. Hama, W. Kunz and R. Buchner, *Phys. Rev. Lett.*, 2005, **95**, 197802.
- 29 D. A. Turton and K. Wynne, *J. Chem. Phys.*, 2008, **128**, 154516.
- 30 C. J. F. Böttcher, *Theory of electric polarization*, Elsevier, Amsterdam, 1973.
- 31 D. A. Turton, D. F. Martin and K. Wynne, *Phys. Chem. Chem. Phys.*, 2010, **12**, 4191–4200.
- 32 D. A. Turton, C. Branca, C. Corsaro, M. Candelaresi, K. R. Seddon, F. Mallamace and K. Wynne, *Faraday Discuss.*, 2011, in press.
- 33 A. Placzek, G. Hefter, H. M. A. Rahman and R. Buchner, *J. Phys. Chem. B*, 2011, **115**, 2234–2242.
- 34 J. Barthel, K. Bachhuber, R. Buchner, H. Hetzenauer and M. Kleebauer, *Ber. Bunsen-Ges. Phys. Chem.*, 1991, **95**, 853–859.
- 35 P. Uhd Jepsen, B. M. Fischer, A. Thoman, H. Helm, J. Y. Suh, R. Lopez and R. F. Haglund, *Phys. Rev. B: Condens. Matter Mater. Phys.*, 2006, **74**, 205103.
- 36 J. Hunger, A. Stoppa, A. Thoman, M. Walther and R. Buchner, *Chem. Phys. Lett.*, 2009, **471**, 85–91.
- 37 P. Lunkenheimer, U. Schneider, R. Brand and A. Loidl, *Contemp. Phys.*, 2000, **41**, 15–36.
- 38 A. Brodin and E. A. Rössler, *J. Chem. Phys.*, 2006, **125**, 114502.
- 39 C. Kalpouzos, W. T. Lotshaw, D. McMorro and G. A. Kenneywallace, *J. Phys. Chem.*, 1987, **91**, 2028–2030.
- 40 H. Cang, V. N. Novikov and M. D. Fayer, *J. Chem. Phys.*, 2003, **118**, 2800–2807.
- 41 D. Xiao, J. R. Rajian, A. Cady, S. F. Li, R. A. Bartsch and E. L. Quitevis, *J. Phys. Chem. B*, 2007, **111**, 4669–4677.
- 42 J. Wiedersich, T. Blochowicz, S. Benkhof, A. Kudlik, N. V. Surovtsev, C. Tschirwitz, V. N. Novikov and E. Rössler, *J. Phys.: Condens. Matter*, 1999, **11**, A147–A156.

-
- 43 R. Richert and C. A. Angell, *J. Chem. Phys.*, 1998, **108**, 9016–9026.
44 M. Anouti, M. Caillon-Caravanier, C. Le Floch and D. Lemordant, *J. Phys. Chem. B*, 2008, **112**, 9412–9416.
45 P. Salvador, J. E. Curtis, D. J. Tobias and P. Jungwirth, *Phys. Chem. Chem. Phys.*, 2003, **5**, 3752–3757.
46 D. Laage and J. T. Hynes, *Science*, 2006, **311**, 832–835.